SEMARAK ILMU PUBLISHING

Journal of Advanced Research in Fluid Mechanics and Thermal Sciences

Journal homepage:
https://semarakilmu.com.my/journals/index.php/fluid_mechanics_thermal_sciences/index
ISSN: 2289-7879

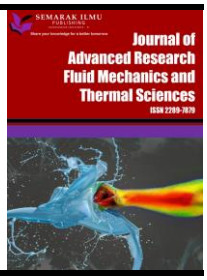

Experimental and Numerical Study on Conical Gravitational Water Vortex Turbine with 3D Runner

Haryadi[1,*], Sugianto[1], Prasetyo[1], Dibyo Setiawan[1]

[1] Department of Mechanical Engineering, Politeknik Negeri Bandung, West Java, Indonesia

ARTICLE INFO

Article history:
Received 1 October 2023
Received in revised form 12 January 2024
Accepted 27 January 2024
Available online 29 February 2024

Keywords:
Conical; GWVT; 3D Runner; low head

ABSTRACT

The gravitational water vortex turbine (GWVT) is a promising solution to exploit the potential of low-head hydro energy. Previous research has shown that a 3D runner performs better than a runner with a flat blade and a 2D curved blade. This research investigates the performance of a conical gravitational water vortex turbine (CGWVT) with a 3D runner using numerical simulations and experiments. The numerical simulations were carried out with Fluent V 6.1, a 2-phase transient incompressible solver, at various torque loads. Furthermore, experiments were conducted to validate the numerical simulations by varying the torque load and water flow rate. The experiment revealed that the maximum power was achieved at a rotational speed of around 100 to 110 rpm. The maximum efficiency was 0.28 at a flow rate of 0.00477 m^3/s. The developed simulation closely matched the experimental results, making it useful for design and prediction for further development.

1. Introduction

Various types of water turbines have been developed to utilize low-head hydro energy. L. O. M. Firman *et al.,* [1] stated that diversification of energy sources stimulates researchers to explore different energy sources, making it a critical aspect of modern society. Some solutions to extract low head hydro energy potential are horizontal spiral turbines, small undershot water wheels, Dethridge wheel, and gravitational water vortex turbines (GWVT). Research indicates that GWVT has advantages over other types of turbines in utilizing low-head hydro energy potential. Sitram and Suntivarakorn [2] conducted an experimental study comparing small undershot water wheels to GWVT and was found that the GWVT was far superior. In addition, gravitational vortex turbines are more stable and can operate with lower heads. Mugisidi *et al.,* [3] proposed a novel Dethridge wheel blade shape, which can achieve an efficiency of 71.7%. However, this performance was achieved at a very low rotational speed of about 13 rpm, which can make it difficult to select a suitable generator. According to Date and Akbarzadeh [4], most of the low-head energy potential has not yet been utilized, and economic considerations are usually the reason for resisting low head hydro energy

* *Corresponding author.*
E-mail address: haryadi.mesin@polban.ac.id

https://doi.org/10.37934/arfmts.114.2.114

utilization. Nonetheless, Guzmán *et al.,* [5] have designed and constructed a 10 kW GWVT for a rural area of Peru with a head of 1 m and the highest test discharge reaching 0.6 m^3/s. This power plant is low-cost and off-grid with the highest efficiency of about 13.9%.

Many studies have been conducted to improve the performance of GWVT. These studies include optimizing the number of blades on the runner, modifying the runner, and optimizing and modifying the basin [6,7]. Initially, vortex turbine blades were flat-radial, but they have been developed into paddle-type, centrifugal, and paddle with baffles [8-11]. Kora *et al.,* [12] proposed a rotated-blade-centrifugal runner. In 2020, preliminary research was carried out to determine the general characteristics of vortex turbines and introduce a new runner with a 3D profile. The 3D runner achieved rotational speeds of up to 190 rpm [13].

According to Wichian and Suntivarakorn [11], the diameter of a hole in a turbine plays a crucial role in determining the torque generated. If the diameter is too small, the tangential velocity of the water will be too low, resulting in low torque generation. Conversely, if the diameter is too large, the water level in the basin will be too low, leading to a decrease in the torque generated. Khan [14] suggests that the optimal basin-to-hole diameter ratio for a turbine is between 0.14 to 0.18.

Dhakal *et al.,* [15] conducted a study on various parameters of a turbine basin, namely: opening, surface height, diameter, and cone angle, using CFD analysis. They compared different basin configurations and concluded that the opening has the greatest impact on the GWVT performance.

In the study conducted by Yadav *et al.,* [16], the potential of increasing the performance of a vortex turbine was investigated by using two runners – a cylinder and a cone simultaneously, positioned at a certain distance from each other. The results revealed that there is an optimum position and distance for the runners that produce the best performance. Similarly, Kayastha *et al.,* [17] conducted a study to determine the impact of different runner positions on the efficiency of a GWVT with a conical basin. The blades of the runner were designed in the shape of a Savonius wind turbine blade. For the simulation, they used ANSYS CFX as the solver with a single phase and utilized a transient solver with a κ-ε turbulent model. The study involved numerical and experimental analysis of a vortex turbine prototype at three different runner height positions. The findings revealed that the runner in the lowest position resulted in the highest rotational speed and best efficiency. The maximum efficiency from experimental analysis was 10.5%, which was slightly different from the simulation results.

Another study by Dakhal *et al.,* [18] investigated the effect of the shape of the vortex basin on the efficiency and output power of a vortex turbine with a paddle type without a bevel. They used CFD simulations and experiments with two basins, namely a cylinder and a cone. To determine the cone angle's effect, the basin's cone angle was varied from 5° to 20°. Calculations with CFD simulations showed that the larger the cone angle, the greater the maximum velocity of the particles in the flow field. This led to the conclusion that the larger the cone angle, the greater the output power. Furthermore, conical basins provide better efficiency than cylindrical ones under the same inlet and outlet conditions.

Bajracharya *et al.,* [19] conducted a study to determine the effect of various geometric parameters on conical basin vortex turbines. They investigated seven sets of runner shapes, each with four types of runners featuring different geometries. The study concluded that the optimal runner height ratio to the basin is between 0.31 to 0.32, the blade taper angle is about 20 degrees, the blade curve angle seen from above is between 50 – 60 degrees, and the cut ratio is not more than 15%. However, none of these runners were 3D.

Aziz *et al.,* [20] conducted a study using a cone-shaped GWVT. The runner used was a flat plate with different angles of inclination. The study also examined the effect of turbine orientation, vertical

and horizontal, on its performance. The results showed that the runner with vertical blades and horizontal orientation generates a higher tangential force.

Saleem *et al.,* [21] conducted a single-level GWVT study using a cylindrical basin and an upright and inclined Savonius runner. It was found that the inclined runner produces a higher efficiency of about 20%.

Suarda *et al.,* [22] observed the performance of semi-twisted blade runners of GWVT and concluded that the GWVT performed better at lower rotation speeds. As the rotational speed of the runner increased, the water level at the top of the basin also increased, which hindered water flow to the basin and ultimately reduced the GWVT performance.

In a study conducted by Ullah *et al.,* [23] the characteristics of a GWVT with a multi-stage conical runner consisting of 3 rotors with 3 different shafts were investigated. The study aimed to improve the extraction of water kinetic energy resulting in higher efficiency. Various parameters, such as torque, rotational speed, and power were examined individually and in combination at each level. The blade profile used was a 3-level Savonius Wind Turbine Blade. The maximum power obtained was about 4.4 Watts, resulting in an efficiency of about 11.9%, with a total head height of 0.94 m and a flow rate of 0.004 m^3/s. It was found that the top runner achieved the highest rotational speed. The research concluded that the use of multilevel runners improves performance due to vortex strengthening caused by rigid body rotations of the inter-stage interaction. The weight of the water above the runners also generates greater torque. However, the interaction between these stages does not always amplify turbine performance because the turbulence generated by the stages above can distort the flow reducing vortex strength and in turn, performance.

A study on the losses that occur in vortex turbines has also been conducted. Nishi *et al.,* [24] used experiments and the free surface flow analysis method. They found that there are three major losses: tank loss, tank outlet loss, and friction loss inside the tank. However, the losses in the runner and friction loss were relatively small. The study also showed that the effective head and the turbine efficiency increase as the flow rate increases. As a result, the turbine output increases at a rate greater than the increase of the flow rate. To build on this research, this study was conducted to investigate the performance of a Conical Gravitational Water Vortex Turbine (CGWVT) with a 3D runner, which was carried out using numerical simulations and experiments.

2. Methodology

Figure 1 shows the nomenclature used for the runner geometry of the CGWVT with a 3D runner. The taper angle refers to the cone angle of the runner as viewed from the front. Blade angle, on the other hand, pertains to the angle of curvature of the blade when viewed from the top. The helix angle, meanwhile, refers to the angle of inclination of the blade twist to the line as seen in the lateral plane of the cylinder. The CGWVT with 3D Runner is a Gravitational Water Vortex Turbine, which consists of a conical basin and an equal tapper angle conical 3D Runner.

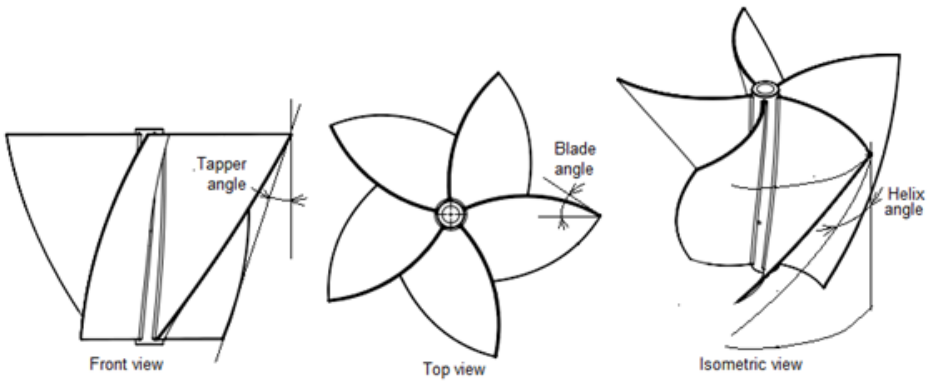

Fig. 1. Blade geometrical nomenclatures

2.1 Runner Design

In this study, the runner was designed in a 3D shape as recommended by Haryadi *et al.,* [13]. The runner consisted of 5 blades as suggested by Sritram and Suntivarakorn [2]. The basin was conical with a 20° taper angle, as recommended by Bajracharya *et al.,* [19]. The runner was in a conical shape. The arrangement of runner geometrical parameters was done based on the recommendation of Bajracharya *et al.,* [19] with some necessary modifications. The picture and model of the conical 3D runner are depicted in Figure 2. The runner height was 240 mm, the blade angle was 60°, the helix angle was 63°, and the tapper angle was 20°. The top diameter was 350 mm, and the mean diameter was 262.7 mm.

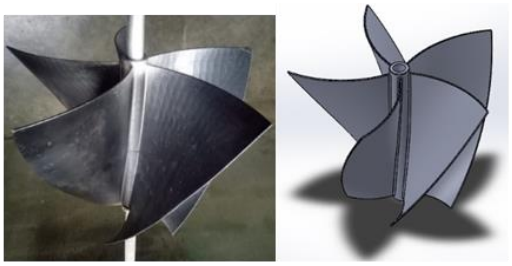

Fig. 2. Picture and model of the conical 3D runner

2.2 Numerical Simulation

Numerical simulations were performed using ANSYS Flow V 6.1, a CFD code with a 3D model, transient, incompressible method. The working fluids were water and air (two phases). The Volume of Fluid (VOF) model was used to solve the free-surface two-phase flow problem. The simulations were conducted under various torque loads. The computational domain, as shown in Figure 3, featured a runner placed in a conical basin. The computational elements were constructed on CGWVT geometry, with homogeneous cell sizes necessary for a two-phase transient flow calculation. The computational elements were hexagonal shapes, with a total of 53,995 cells, as seen in Figure 4.

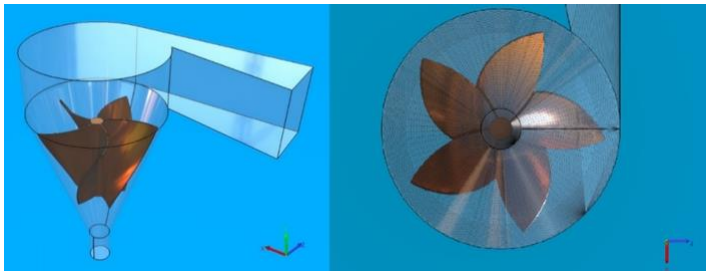

Fig. 3. Computational simulation domain

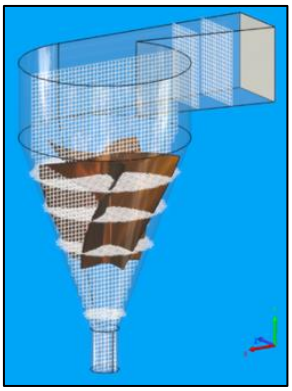

Fig. 4. Computational elements, as seen from some planes

Numerical simulations were conducted using dynamic fluid-body coupling interactions. In this transient-incompressible solver, the flow of a two-phase water-air fluid applies pressure or force on the runner's surface. The shaft and runner assembly were assumed uniform. This interaction causes the runner to rotate on its axis (one degree of freedom). The fluid properties are described in Table 1, while the boundary and initial conditions are described in Table 2. The external torque in the y-axis direction was used as the load model.

Table 1
Fluid properties

	Property	Value	Unit	Remarks
Water	Density	998.3	kg/m^3	
	Viscosity	0.001	Pa.s	
Air	Density ρ	1.225	kg/m^3	
	Viscosity	1.7894xE-5	Pa.s	
Water-air	Surface tension	0.072	N/m	
interactions	Contact angle	90	°	
	Runner revolution	0	rpm	
Runner, shaft,	Revolution direction (x, y, z)	(0,1,0)	-	The rotation
bearing (solid,				axis is y+
homogenous	Translation direction (x, y, z)	(0,0,0)	-	No translation
assumed)	Mass	3.39	kg	-
	Gravity	9.81	m/s^2	y- direction
Load model on	External moment	0.172;	N.m	Y- direction
the shaft		0.329;		
		0.495;		
		0.645;		
		0.707;		
		0.801		

Table 2
The boundary and the initial conditions

	Parameter	Value	Unit
Boundary conditions	Debit	4.77	Liter/s
	Pressure	1	atm
	Courant number	1	
	Roughness basin	0	m
Initial conditions	Water fraction	0	-
	Runner revolution	0	rpm
Solver	Transient	-	-
	incompressible	-	-

2.3 Experimental Setup

The test installation primarily comprises a conical basin with a runner and consists of an open channel, plenum reservoir, and pump. Figure 5 shows a schematic of the experimental setup. The main components of the experimental apparatus are a vortex basin with a 3D conical runner, an open channel, a Prony brake with a torque meter, and an ultrasonic flow meter. The ultrasonic flow meter was calibrated by filling the reservoir with water and recording the time taken for the process using a stopwatch. The rotational speed was measured using a digital laser tachometer.

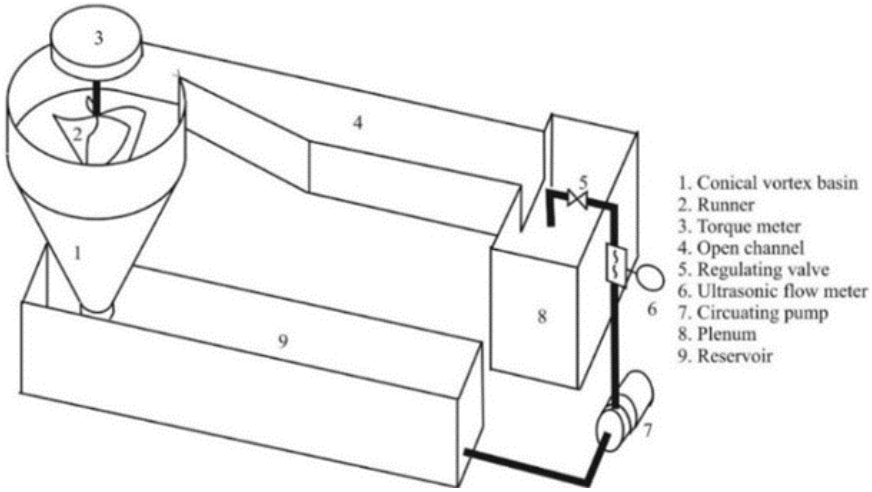

Fig. 5. Experiment setup and apparatus

The torque meter consists of pulleys, a band, two load cells, and a load. By moving along the rod, the rod can be balanced. Experiments were conducted at various constant water debits, with the load W being varied at each water debit. The water debit was controlled using a ball valve. Then, the load W was applied, and after reaching a steady state, the shaft rotation speed was measured, and the forces on both sides of the band were recorded using the load cell. Still at the same water debit, the load W was changed to obtain the rotational speed and forces on the two sides of the band. The obtained mechanical power was calculated using the following equations:

$$P_m = \frac{2\pi}{60} NT \tag{1}$$

$$T = r(F_1 - F_2) \tag{2}$$

where N is the rotational speed, T is the torque, r is the pulley radius, and F_1 and F_2 are the forces on the two sides of the band, respectively.

Furthermore, the water level in the waterway was also recorded, and the hydraulic power was determined by the following equation:

$$P_h = \rho g Q H \tag{3}$$

where ρ is the density of water, g is the gravity acceleration, Q is the debit and H is the head (m) which is the difference between the water level of the waterway and the end conical basin. The stated efficiency of the vortex turbine is:

$$\eta = P_m / P_h \tag{4}$$

3. Results

3.1 Numerical Simulation Result

Figure 6 shows the numerical simulation results curve of angular velocity at the water debit of 0.0047 m³/s, with a constant torque load of 0.645 Nm. The graph indicates that the angular velocity gradually increases with a relatively large gradient at the beginning when the volume of water touching the turbine blade surface increases. The turbine starts rotating at 0.6 seconds, and the rotational speed increases rapidly. After 5 seconds, the rotational speed increases slowly until it reaches a steady state. The rotational speed curve exhibits ripples which occur due to the momentum pulsation caused by the limited number of blades. So far, this phenomenon has not been observed in experimental measurements yet.

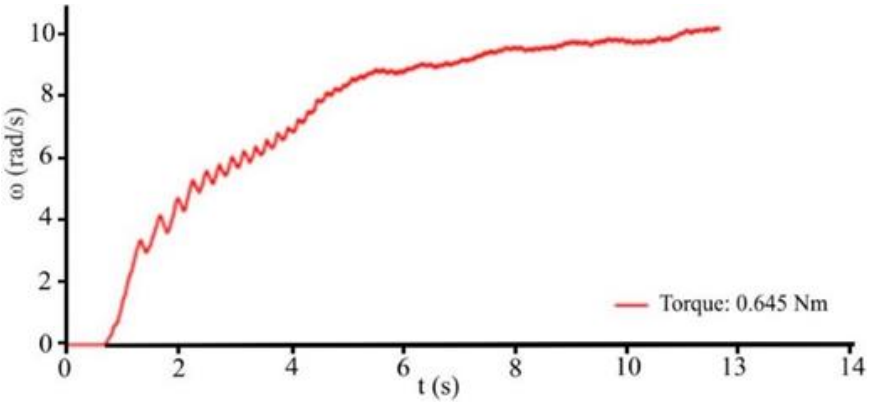

Fig. 6. Angular velocity against time at torque load 0.645 Nm and 0.00477 m³/s flow rate

The simulation provided the VOF fraction of each computational cell. A VOF fraction of 1 indicates that the cell is filled with water, while a VOF fraction of zero indicates that the cell is filled with air. The free surface can be identified by cells with 0.5 < VOF < 1. Figure 7 shows a comparison of the free surface obtained from the simulation and the experiment between 0.2 and 11 s. Up to 0.3 seconds, the water is still flowing from the open channel to the turbine chamber, causing the turbine to remain at rest as shown in Figure 7. At 0.4 seconds, the water flow begins to enter the turbine chamber, and at 0.6 seconds, it touches the surface of the turbine blade.

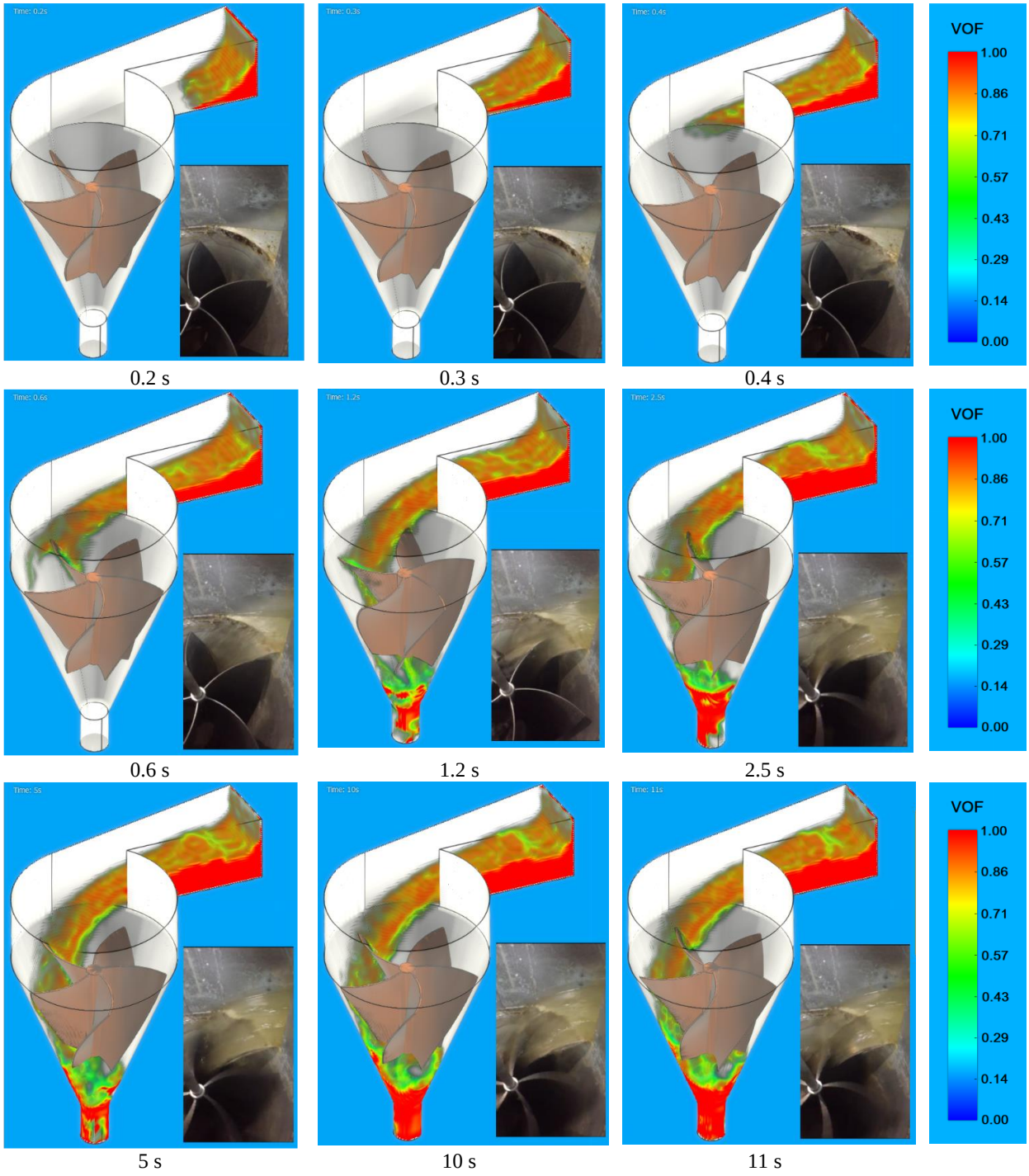

Fig. 7. VOF fraction from t = 0.2 to 11 s

Furthermore, until the time of 1.2 seconds, the turbine rotational speed increases rapidly, as shown in Figure 6. From 1.2 to 5 seconds, the gradient of increase in turbine rotational speed decreases. The turbine rotational speed remains constant from 5 to 11 seconds when the water flow into the basin becomes steady. The simulation results indicate that the free surface is similar to the experimental results. As shown in Figure 11, by 11 seconds, the rotational speed approaches a steady state.

In Figure 10, it can be observed that the vorticity of 40 s^{-1} is an average vorticity that dominates and can represent other vorticities. Figure 8 shows the VOF fraction on the surface vorticity of 40 s^{-1} for the two-phase water-air flow of GWVHT with a debit of 0.00477 m^3/s and a time of 11 seconds.

The figure indicates that a vortex also occurs in the air phase. At the top layer, the VOF is equal to zero, and the zero VOF dominates, indicating that even in conditions that are close to steady, the air phase still occupies most of the basin space. Thus, numerical simulations of vortex turbines should indeed be conducted in two phases – air and water. Compared with Figure 6, it can be concluded that even though the water has entered the basin at t=11 seconds, the vorticity is still likely to be less than 40 s^{-1} and hence not visible in Figure 8. The figure also demonstrates that the fluid flow under the runner has a vorticity of 40 s^{-1}, which is dominated by the water phase.

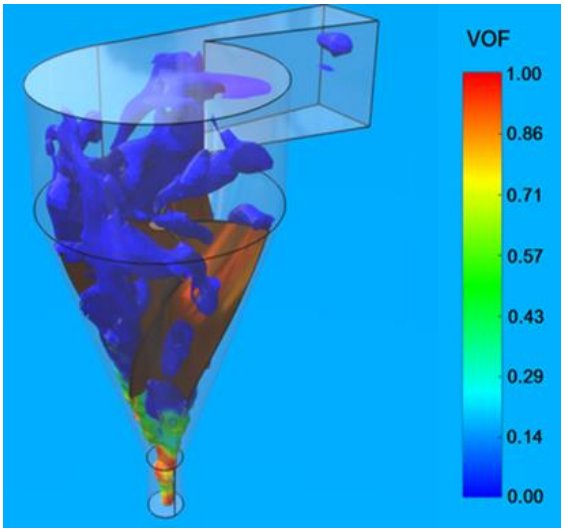

Fig. 8. VOF fraction on the iso-surface vorticity of 40 s^{-1} the debit of 0.00477 m^3/s and time of 11 s

Figure 9 illustrates the velocity distribution of the fluids at the four different planes in the basin when the water debit is 0.00477 m^3/s and the time is 11 seconds. At the top plane, the fluid velocity appears to be generally quite low, ranging between 0 and about 1.3 m/s. This is because there is no runner blade present, which means it does not contribute directly to the formation of torque. However, at the second plane, the average speed is increasing although it is still seen that the speed is low in the near shaft area caused by the whirl. In the third plane, located below the runner, the fluid velocity increases, which is partly due to the reduced cross-sectional area. Finally, in the fourth plane, the average water velocity is about 2.6 m/s which is more or less the same as the velocity of water through the orifice due to the water column.

Figure 10 shows the distribution of the vortex's strength or vorticity in a two-phase water-air flow in open channels and basins. The figures reveal that even though some areas are not filled with water, the cells with a VOF fraction equal to zero still dominate the space. It can be concluded that the turbine power can be further increased by either flowing more water or optimizing the geometry of the basin and runner. Moreover, the vorticity is getting higher at the bottom, indicating that the use of a conical basin can increase the vortices. Although the vortices in the initial segments appear large and disappear when the water returns to the inlet, the vorticity between segments is relatively consistent in the middle and lower areas.

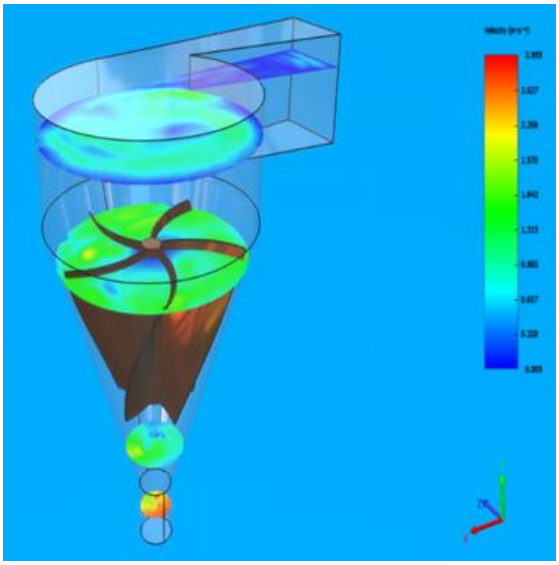

Fig. 9. Velocity at the plane 2 phase water-air flow at the debit of 0.00477 m^3/s and time of 11 s

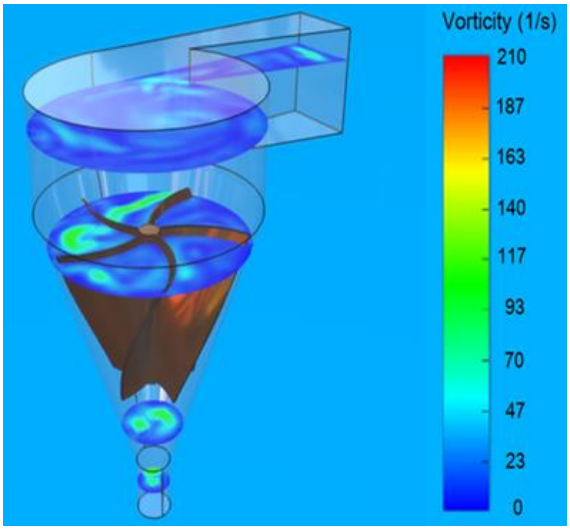

Fig. 10. Vorticity for several cross sections at t = 11 s

Figure 11 illustrates the angular velocity of the runner against the time at different torque loads from numerical simulation. All curves display a similar trend. At the beginning of the fluid flow, the runner is still at rest until 0.35 seconds, after which it begins to rotate as the working fluid pushes the blade and gradually increases the angular speed of the runner as the mass of the flowing fluid increases. The increase in runner angular speed is relatively the same for all torque loads in the time range of 0 - 1.2 seconds, except for the torque load of 0.810 Nm, which is fairly low. The runner's rotational speed continues to increase with different gradients until t = 4 seconds, after which it starts to slope towards steady fluid flow conditions, where the incoming fluid's mass flow rate equals the fluid's mass leaving the hole. It is also observed that the runner's rotational speed decreases with increasing torque load, which moves against the direction of the runner's rotation. The curves show ripples, with the height getting smaller with time due to pulsation caused by the free space between the blades. For the torque load of 0.810 Nm, the blade rotation tends to be unstable, caused by the amplification of the ripple at a very low angular speed. At this condition, the average angular speed

from the numerical simulation was 9.5 rad/s, while from the experiment was 16.8 rad/s (44 rpm). This was because of the simulations have not yet reached fully steady, as explained later.

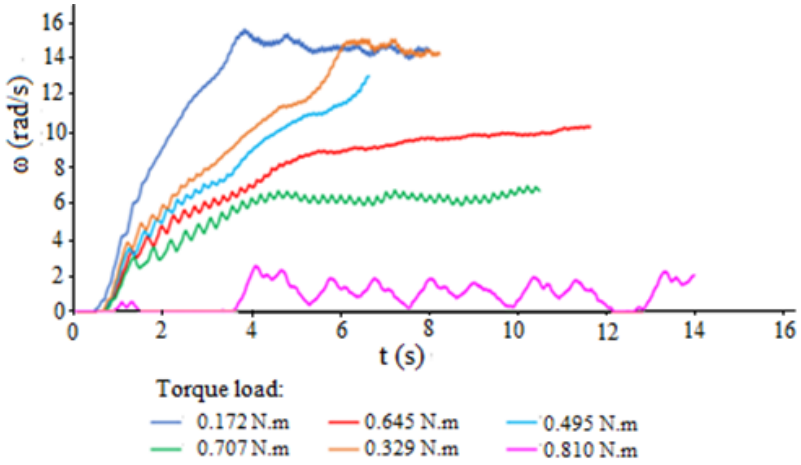

Fig. 11. Angular speed against time at various torque loads and 0.00477 m³/s flow rate from simulation

3.2 Experiment Result

Figure 12 shows a graph that plots the shaft power against the rotational speed at different flow rates. The graph indicates that the highest power output of 6.8 watts is achieved at a flow rate of 0.00477 m³/s when the rotational speed is at around 95 to 110 rpm. At a flow rate of 0.00404 m³/s, the maximum power output of 5.1 is achieved at a rotation of about 100 to 115 rpm. The maximum power at a flow rate of 0.00477 m³/s was 6.8 watts, while at a flow rate of 0.00404 m³/s, the maximum power was 5.1 watts. Maximum power tends to decrease with decreasing flow rate. The water only partially inundates the basin at a low flow rate. It was seen during the experiment that at a low flow rate, the water was empty in the middle of the basin. The figure also shows that the maximum efficiency peak does not shift from the area between 100 – 110 rpm indicating that the flow pattern tends to be the same.

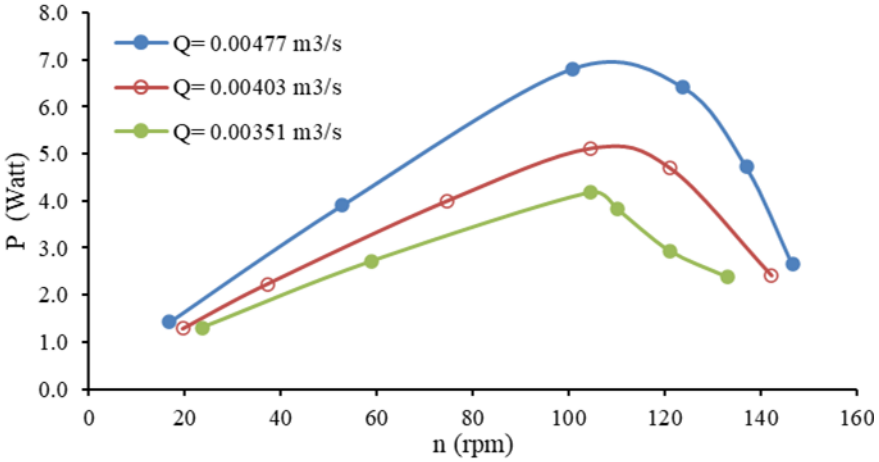

Fig. 12. Shaft power against rotational speed

Figure 13 shows a graph of efficiency against rotational speed. The efficiency referred to here is the ratio of shaft power to hydraulic power. The hydraulic power is calculated using the head, the difference between the height of the water level in the open channel, and the water level at the

turbine tail race. It can be seen in Figure 13 that the maximum efficiency that can be achieved is 0.28, which is much higher than that of the 3-stage conical runner, which is estimated at 0.11. The graph also shows that the efficiency at a flow rate of 0.00477 m³/s is generally slightly higher than that at a flow rate of 0.00403 m³/s. Compared to the 3D cylinder, which achieved an efficiency of 23.8%, the conical design is considerably more efficient.

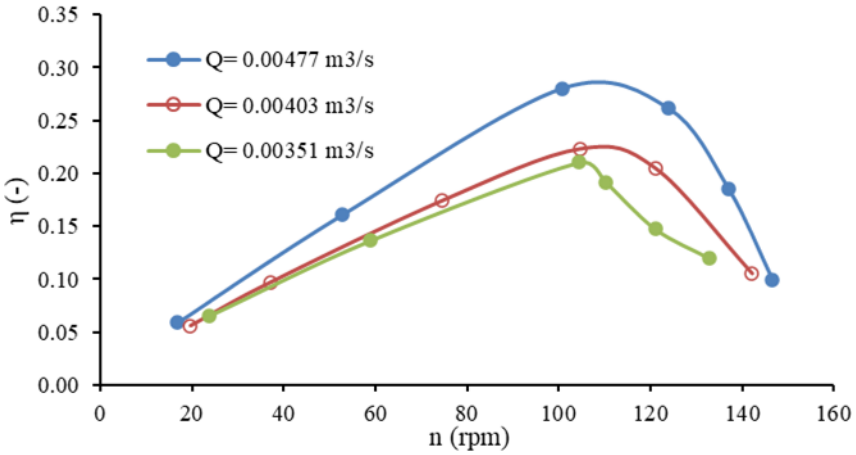

Fig. 13. Efficiency against rotational speed

Figure 14 shows a graph of efficiency against rotational speed. The efficiency referred to here is the shaft power divided by the hydraulic power. The hydraulic power is calculated using the head, the difference between the height of the water level in the open channel, and the water level at the turbine tail race. The graph indicates that the maximum efficiency that can be achieved is 0.28, which is much higher than that of the 3-stage conical runner, which is estimated at 0.11. The graph also reveals that the efficiency is generally slightly higher at a flow rate of 0.00477 m³/s than at a flow rate of 0.00403 m³/s. Compared to the 3D cylinder, which reached 23.8%, the efficiency of the 3D conical is also much higher. During the experiment, the shaft powers obtained were higher than those of the numerical simulation at almost all torque load values. This was because the simulations did not yet reach a fully steady state due to the computational capacity limitation of the iteration duration. For the two highest torque values, the shaft powers obtained from the experiment were smaller than those of the numerical simulation, probably because of the presence of mechanical friction in the experiment.

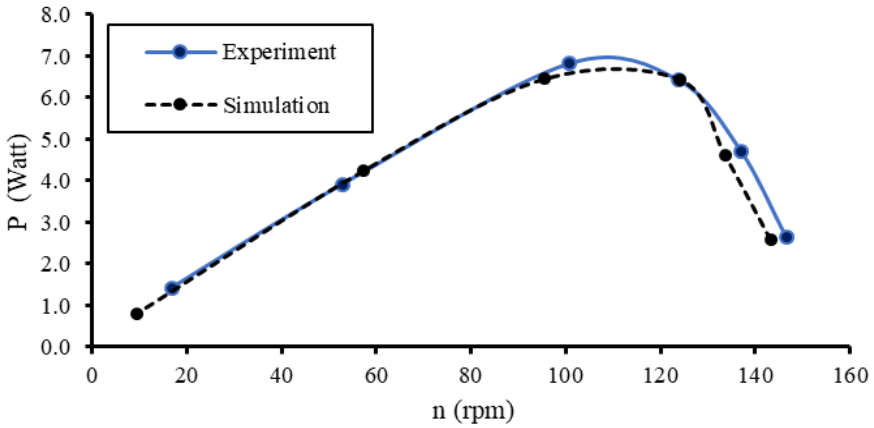

Fig. 14. Comparison of shaft power obtained from simulation and experiment

4. Conclusions

The Conical Gravitational Water Vortex Turbine (CGWVT) with 3D runner has been developed and tested. The maximum power is achieved at around 95 to 110 rpm when the flow rate is 0.00477 m^3/s, while at a flow rate of 0.00404 m^3/s, the maximum power is reached at a rotation of about 100 to 115 rpm. Comparison with the 3D cylindrical runner shows that this 3D conical runner is better. At a flow rate of 0.00477 m^3/s, the maximum efficiency was 0.28. The shaft power obtained from the developed simulation is quite close to the experimental results.

The numerical calculations successfully predicted the angular velocity, water-free surface pattern, and turbine performance. Therefore, the behaviour of CGWVT can be simulated by numerical methods that have been developed. Even though there is still air-filled space in the GWVT basin, turbine power can still be increased by accelerating the flow rate or improving the surface curve of the runner blade.

Acknowledgement

The authors are grateful to P3M, Politeknik Negeri Bandung, for grant number B/78.4/PL1.R7/PG.00.03/2021 to finance this research.

References

[1] Firman, La Ode Mohammad, Rizky Bayu Adji, and Reza Abdu Rahman. "Increasing the feasibility and storage property of cellulose-based biomass by forming shape-stabilized briquette with hydrophobic compound." *Case Studies in Chemical and Environmental Engineering* 8 (2023): 100443. https://doi.org/10.1016/j.cscee.2023.100443

[2] Sritram, Piyawat, and Ratchaphon Suntivarakorn. "Comparative study of small hydropower turbine efficiency at low head water." *Energy Procedia* 138 (2017): 646-650. https://doi.org/10.1016/j.egypro.2017.10.181

[3] Mugisidi, Dan, Irfan Nur Fauzi, Oktarina Heriyani, Yusuf Djeli, Erwin Aidhilhan, and Pancatatva Hesti Gunawan. "Development of the Dethridge Wheel Blade Shape for Hydropower Generation in Irrigation Canals in Indonesia." *Journal of Advanced Research in Fluid Mechanics and Thermal Sciences* 98, no. 2 (2022): 146-156. https://doi.org/10.37934/arfmts.98.2.146156

[4] Date, Abhijit, and Aliakbar Akbarzadeh. "Design and cost analysis of low head simple reaction hydro turbine for remote area power supply." *Renewable Energy* 34, no. 2 (2009): 409-415. https://doi.org/10.1016/j.renene.2008.05.012

[5] Guzmán, Vladimir J. Alzamora, Julie A. Glasscock, and Ferris Whitehouse. "Design and construction of an off-grid gravitational vortex hydropower plant: A case study in rural Peru." *Sustainable Energy Technologies and Assessments* 35 (2019): 131-138. https://doi.org/10.1016/j.seta.2019.06.004

[6] Sritram, P., and R. Suntivarakorn. "The effects of blade number and turbine baffle plates on the efficiency of free-vortex water turbines." In *IOP Conference Series: Earth and Environmental Science*, vol. 257, no. 1, p. 012040. IOP Publishing, 2019. https://doi.org/10.1088/1755-1315/257/1/012040

[7] Velásquez, Laura, Alejandro Posada, and Edwin Chica. "Optimization of the basin and inlet channel of a gravitational water vortex hydraulic turbine using the response surface methodology." *Renewable Energy* 187 (2022): 508-521. https://doi.org/10.1016/j.renene.2022.01.113

[8] Power, Christine, Aonghus McNabola, and Paul Coughlan. "A parametric experimental investigation of the operating conditions of gravitational vortex hydropower (GVHP)." *Journal of Clean Energy Technologies* 4, no. 2 (2016): 112-119. https://doi.org/10.7763/JOCET.2016.V4.263

[9] Dhakal, Sagar, Ashesh B. Timilsina, Rabin Dhakal, Dinesh Fuyal, Tri R. Bajracharya, Hari P. Pandit, Nagendra Amatya, and Amrit M. Nakarmi. "Comparison of cylindrical and conical basins with optimum position of runner: Gravitational water vortex power plant." *Renewable and Sustainable Energy Reviews* 48 (2015): 662-669. https://doi.org/10.1016/j.rser.2015.04.030

[10] Nishi, Yasuyuki, Daichi Sukemori, and Terumi Inagaki. "Performance and Flow Field of Gravitation Vortex Type Water Turbine using Volute Tank." *International Journal of Fluid Machinery and Systems* 14, no. 3 (2021): 229-246. https://doi.org/10.5293/IJFMS.2021.14.3.229

[11] Wichian, Pongsakorn, and Ratchaphon Suntivarakorn. "The effects of turbine baffle plates on the efficiency of water free vortex turbines." *Energy Procedia* 100 (2016): 198-202. https://doi.org/10.1016/j.egypro.2016.10.165

[12] Kora, Amanuel Tesfaye, Venkata Ramayya Ancha, and Getachew Shunki Tibba. "Numerical analysis of the effect of runner-to-basin diameter ratio on the performance of gravitational water vortex turbine in a scroll basin." *International Journal of Energy and Environmental Engineering* 13, no. 4 (2022): 1317-1333. https://doi.org/10.1007/s40095-022-00495-4

[13] Haryadi, Haryadi, Adri Maldi Subarjah, and Sugianto Sugianto. "Experimental study on 3D vortex gravitational turbine runner." In *AIP Conference Proceedings*, vol. 2296, no. 1. AIP Publishing, 2020. https://doi.org/10.1063/5.0030545

[14] Khan, Nauman Hanif. "Blade optimization of gravitational water vortex turbine." *PhD diss., Tesis MT, Teknik Mesin, Ghulam Ishaq Khan Institute of Engineering Sciences and Technology* (2016).

[15] Dhakal, Sagar, Ashesh Babu Timilsina, Rabin Dhakal, Dinesh Fuyal, Tri Ratna Bajracharya, and Hari Prasad Pandit. "Effect of dominant parameters for conical basin: Gravitational water vortex power plant." In *Proceedings of IOE Graduate Conference*, vol. 5, p. 381. 2014.

[16] Yadav, Bharosh Kumar, Amit Chandra Jyoti, Pintu Kr Rajak, Ramesh Kr Mahato, Deelip Kr Chaudhary, Mehdi Jahangiri, and Ram Dayal Yadav. "CFD Analysis of the Most Favorable Gap Between the Main Runner and Booster Runner of Gravitational Water Vortex Turbine." *Journal of Renewable Energy and Environment* 9, no. 2 (2022): 75-81.

[17] Kayastha, Manil, Prashant Raut, Nirmal Kumar Subedi, Sandesh Tamang Ghising, and Rabin Dhakal. "CFD evaluation of performance of Gravitational Water Vortex Turbine at different runner positions." *KEC Conference* (2019): 17-25. https://doi.org/10.31224/osf.io/d9qn3

[18] Dhakal, Sagar, Ashesh B. Timilsina, Rabin Dhakal, Dinesh Fuyal, Tri R. Bajracharya, Hari P. Pandit, Nagendra Amatya, and Amrit M. Nakarmi. "Comparison of cylindrical and conical basins with optimum position of runner: Gravitational water vortex power plant." *Renewable and Sustainable Energy Reviews* 48 (2015): 662-669. https://doi.org/10.1016/j.rser.2015.04.030

[19] Bajracharya, Tri Ratna, Shree Raj Shakya, Ashesh Babu Timilsina, Jhalak Dhakal, Subash Neupane, Ankit Gautam, and Anil Sapkota. "Effects of geometrical parameters in gravitational water vortex turbines with conical basin." *Journal of Renewable Energy* 2020 (2020): 1-16. https://doi.org/10.1155/2020/5373784

[20] Aziz, Muhammad Qamaran Abdul, Juferi Idris, and Muhammad Firdaus Abdullah. "Simulation of the Conical Gravitational Water Vortex Turbine (GWVT) Design in Producing Optimum Force for Energy Production." *Journal of Advanced Research in Fluid Mechanics and Thermal Sciences* 89, no. 2 (2022): 99-113. https://doi.org/10.37934/arfmts.89.2.99113

[21] Saleem, Abdul Samad, Taqi Ahmad Cheema, Rizwan Ullah, Sarvat Mushtaq Ahmad, Javed Ahmad Chattha, Bilal Akbar, and Cheol Woo Park. "Parametric study of single-stage gravitational water vortex turbine with cylindrical basin." *Energy* 200 (2020): 117464. https://doi.org/10.1016/j.energy.2020.117464

[22] Suarda, Made, Made Sucipta, and Ibnu Gusti Muttakin. "Semi Twisted Curve Blade Vortex Turbine Performance at Runner Rotation Speed Variation using CFD Simulation." *Journal of Advanced Research in Fluid Mechanics and Thermal Sciences* 104, no. 2 (2023): 26-35. https://doi.org/10.37934/arfmts.104.2.2635

[23] Ullah, Rizwan, Taqi Ahmad Cheema, Abdul Samad Saleem, Sarvat Mushtaq Ahmad, Javed Ahmad Chattha, and Cheol Woo Park. "Preliminary experimental study on multi-stage gravitational water vortex turbine in a conical basin." *Renewable Energy* 145 (2020): 2516-2529. https://doi.org/10.1016/j.renene.2019.07.128

[24] Nishi, Yasuyuki, Ryouta Suzuo, Daichi Sukemori, and Terumi Inagaki. "Loss analysis of gravitation vortex type water turbine and influence of flow rate on the turbine's performance." *Renewable Energy* 155 (2020): 1103-1117. https://doi.org/10.1016/j.renene.2020.03.186